IEEE Access
Multidisciplinary | Rapid Review | Open Access Journal

Received January 31, 2019, accepted March 14, 2019, date of publication March 19, 2019, date of current version April 5, 2019.

Digital Object Identifier 10.1109/ACCESS.2019.2906244

Manifold Alignment via Global and Local Structures Preserving PCA Framework

TIMOTHY APASIBA ABEO[1,2], XIANG-JUN SHEN[1], ERNEST DOMANAANMWI GANAA[1,3], QIAN ZHU[1], BING-KUN BAO[4], (Member, IEEE), AND ZHENG-JUN ZHA[5], (Member, IEEE)

[1]School of Computer Science and Communication Engineering, Jiangsu University, Zhenjiang 212013, China
[2]School of Applied Science, Tamale Technical University, Tamale, Ghana
[3]School of Applied Science, Wa Polytechnic, Wa, Ghana
[4]Nanjing University of Posts and Telecommunications, Nanjing 210003, China
[5]School of Information Science and Technology, University of Science and Technology of China, Hefei 230022, China

Corresponding author: Xiang-Jun Shen (xjshen@ujs.edu.cn)

This work was supported in part by the National Natural Science Foundation of China under Grant 61572240, Grant 61622211, and Grant 61872424, and in part by the Senior Talent of Jiangsu University under Grant 14JDG189.

ABSTRACT Manifold alignment is very prevalent in machine learning for extracting common latent space from multiple datasets. These algorithms generally aim to achieve higher alignment accuracies by preserving the original structure while ensuring closeness between manifolds. This paper proposes a novel semi-supervised manifold alignment method that combines, in each manifold, both global and local linear reconstructions. We preserve a local structure through multiple manifold embedding methods. Moreover, we view manifold embedding methods as special forms of principal component analysis (PCA) and, thus, present a new penalty weight PCA approach to preserving a noise-free global structure. Finally, a closed-form solution is presented in the manifold alignment. This method can concurrently match the pair-wise correspondence and preserve both the global and local structures of each dataset to obtain a latent low-dimensional space. The extensive experiments on manifold alignment prove that the proposed method achieves significantly better alignment results than the comparative methods.

INDEX TERMS Correspondence information, global structure, local structure, manifold alignment, manifold learning, PCA, semi supervise.

I. INTRODUCTION

There is prevalence of high dimensional multiple datasets with a common latent space in most fields of computer vision, data mining, and pattern recognition. For example, texts in different languages of the same document, images from different angles of the same object, images and texts from the same document, etc. But aligning these multiple datasets of different features [1] in high dimensionality is very challenging. Therefore, transforming these datasets to a latent low-dimensional space has become urgent [2], [3].

Manifold alignment techniques capable of obtaining a latent low-dimensional space from multiple datasets [4]–[6] have been presented. A general objective of these techniques is to discover manifold structures, build connections and map all input datasets towards a common latent low-dimension space. Representative methods include; manifold alignment using procrustes analysis (PAMA) [4], semi-supervised manifold alignment (SSMA) [5], local non-linear alignment (LNA) [7], unsupervised manifold alignment (UNMA) [6], low rank alignment (LRA) [2], semi-supervised manifold alignment based on local structure preservation (SLLR) [8], and manifold alignment preserving global geometry (PGGMA) [9]. These techniques are usually performed at the level of features or instances. At the feature-level [9], mapping functions are normally computed from the input datasets to obtain the latent space. While embedding coordinates of the input data points are computed at instance-level [4].

In pursuit of most manifold alignment methods to preserve the original structure of each dataset, manifold embedding methods [10]–[12] are used. These manifold embedding methods have shown successes in obtaining low-dimensional spaces [13], [14] in various fields where data points lie on single manifolds. Methods such as Sparse PCA [15] and Linear Discriminant Analysis (LDA) [16] preserve global structures. Whereas Joint Graph Sparse Coding (JGSC) [17],

The associate editor coordinating the review of this manuscript and approving it for publication was Bora Onat.

Neighborhood Preserving Embedding (NPE) [18], Laplacian Eigenmaps (LE) [19], and Locality Preserving Projections (LPP) [20] are local structure preserving techniques. In contrast, Zhu *et al.* [21] presented a method to preserve local and global structures for feature selection. Despite the contributions of the existing manifold alignment methods, structural preservation receive little attention. But in those few instances, only local structure is preserved using single manifold embedding methods [22]. This makes generalization across different input datasets or application areas very challenging.

This paper proposes a semi-supervised framework called **manifold alignment via global and local structures preserving PCA framework (MAPGL)**. It describes manifold structure using correspondences between the datasets and the geodesic distances of the data points. A close-form solution is presented that optimally maps to a common latent low-dimensional space with sufficient information of the input multiple datasets. Specifically, we employ multiple manifold embedding methods to preserve more refined local structure, and noise-free global structure preserve through a penalty weight PCA approach. To present it more clearly, different from the related algorithms such as SSMA and SSMA-FC, the contributions of this paper are in fourfold.

(1) We present an optimal evaluation of multiple manifold embedding methods to preserve local structures of each dataset. This provides more relevant and diverse information than the existing approach of using a single manifold embedding method.
(2) In addition, a new penalty weight PCA is incorporated to guarantee re-discovery and retention of vital data points in preserving global structures of each dataset. This addresses the problem (example, in cross-language retrieval) where global geometry of data is very necessary.
(3) We prove that manifold embedding methods are special forms of PCA, and thereby formulate both into a unified PCA framework. Thus a balance of global and local structures in MAPGL gives more refined, generalized and stable manifold structure robust to noise.
(4) Finally, through a close-form solution, the connection between manifolds together with their global and local manifold structures, are simultaneously optimized to obtain a common latent low-dimension space with sufficient information of multiple datasets.

Extensive experiments on manifold alignment demonstrate the effectiveness of our proposed framework over the comparative PAMA, UNMA, SSMA, and SSMA-FC methods. In the rest of this paper, related works are reviewed in Section II. The proposed methodology is discussed in Section III. In Section IV we present experimental results and finally conclude in Section V.

II. RELATED WORK

This section presents a review and recent progress on manifold alignment. Methods of manifold alignment existed over a decade with the very early approaches being semi supervised [5], [23]. These approaches generally achieve latent spaces through prior knowledge of correspondence information between the different datasets. Following, an approach termed semisupervised alignment of manifolds (SSMA) [5] was presented. And it considers the preservation of local geometry together with a match of close embedded coordinates of the points in correspondence. From a different perspective, an algorithm for preserving global geometry [9] was presented. This approach achieves better performance than those preserving local geometry, in areas where global geometry is a necessity. An algorithm was presented based on hypergraph [24] to map users across networks. By using hypergraphs and prior information of correspondence, different network users are mapped to a common latent space. Also based on hypergraph, a framework termed unified manifold alignment on hypergraph (UMAH) [25] was recently proposed to map common users across social networks. Zhou *et al.* [26] proposed a semi-supervised manifold alignment for indoor localization base on graph construction termed GrassMA, to obtain a radio map with few labeled fingerprints in a cost-efficient way. The GrassMA approach shows enhance robustness to environmental changes in indoor wireless local area network (WLAN).

Zhang *et al.* [27] presented a comparison of local methods for face alignment. Based on a given general framework of local face alignment, they studied and compared three methods to inform interested readers about new cues. A method of shared manifold from a probability theory perspective has been presented by Verbeek [28]. The method has a limitation of modeling multi-modal conditions, due to its one-to-one mappings nature. Yang and Crawford [29] presented a manifold alignment method termed, a joint manifold with global-local preservation (GLMA) for classification of multi temporal hyper spectral images. GLMA aligns global temporal data manifolds at the same time incorporates local point relations to take care of local scale. To handle the problem of aligning remote sensing images in different modalities, Tuia *et al.* [30] presented a semisupervised manifold alignment (SS-MA) method. SS-MA gathers together samples of the same and disperses those of unlike class, thus a latent space with like images is achieved. Stitching of multiview images require the transfer of color to avoid inconsistencies among views, lightening conditions, etc for a seamless stitching. Thus, Qian *et al.* [31] presented a manifold alignment method. This method projects both source and target images to a shared embedding space, preserving both local geometries and corresponding pixels of the overlapped area.

To handle situations where it is impossible to identify corresponding pairs, a semi-definite [32] approach was proposed. This approach formulates a semi-definite programming problem by considering relative comparison information between datasets. A Distribution Adaptation and Manifold Alignment (DAMA) [33] was presented for the detection of fault in cross-domain. This method obtains a low-dimensional subspace where shifts in structure and

distribution are simultaneously reduced by mapping monitoring data of source and target domains. Procrustes analysis was used for alignment of manifold (PAMA) [4]. PAMA is a typical two-steps approach: it first maps the instances to lower dimensions using LE [19] or LPP [20], and then the two embedding spaces are aligned using Procrustes analysis. A one-step algorithm similar to SSMA but considers few correspondences (SSMA-FC) [22] was presented, which builds connections between manifolds differently from SSMA. SSMA-FC builds connections of all points into the cost function, rather than only the predetermined correspondences as in SSMA. Also presented is a method of manifold alignment based on preserving local structure (SLLR) [8]. SLLR obtains a common intrinsic structure through matching instances of correspondence and preserving local structure of each manifold. Zhao *et al.* [34] presented a framework of multi-view manifold learning with locality alignment (MVML-LA). This framework can obtain low-dimensional latent space in supervised and unsupervised multi-view scenarios. This method enhances discrimination of the latent space with locality alignment. To deal with non-linear dimension reduction, Niu and Ma [7] proposed a local non-linear alignment (LNA) from local pull-back concept and a manifold mathematical characteristic. LNA presented a mathematical derivation of the relation between global and local coordinates, which is flexible and non-linear. To predict software proneness to defects, a multi-source selection based manifold discriminant alignment [35] technique was presented. Further, Jing *et al.* [36] presented a method to solve the problem of within-project and cross-project class-imbalance in software defect prediction. Also, a semi-supervised dictionary learning method [37] has been presented for both cross-project and within-project semi-supervised defect predictions.

From the preceding discussion, it is evident that most manifold alignment approaches rely on graph embedding methods to enhance their alignment accuracies. The fundamental idea of graph embedding methods [38], [39] is to construct an approximate affinity graph to a data manifold and through preserving the graph structure, learn a low-dimension space of the data. Representative methods include locality preserving projections [20], laplacian eigenmap [19] and neighborhood preserving embedding [18].

The proposed MAPGL is a one-step alignment method, which solves an optimization problem similar to SSMA and SSMA-FC to obtain a low embedding. On the contrary, this paper is very different in preserving structures of each dataset: While the existing methods preserve local structures using a single graph, MAPGL uses multiple local graphs. In addition, global structures are preserved using a PCA-like approach which enhances the robustness in a wide range of application domains.

III. THE PROPOSED MAPGL METHOD

Consider two available datasets $X = [x_1, x_2, \cdots, x_m] \in \Re^{N_x \times m}$ and $Y = [y_1, y_2, \cdots, y_n] \in \Re^{N_y \times n}$. Where $x_i \in \Re^{N_x}$ and $y_j \in \Re^{N_y}$ are sample column vectors from the original d-dimensional manifolds x and y. N_x and N_y represent the numbers of features in the manifolds, while m and n are the numbers of data points. For problems of semi-supervised manifold alignment, we consider some sample points as pairwise correspondences. Without distorting the original structure, assume $m \leq n$ or $n \leq m$, a pair of correspondence $x_i \leftrightarrow y_j, i = 1, \cdots, c$ exists such that x_i and y_j possess identical latent features. The aim of our algorithm is to respectively map X and Y to embedding coordinates $k = [k_1, \cdots, k_m] \in \Re^{d \times m}$ and $t = [t_1, \cdots, t_n] \in \Re^{d \times n}$, or the linear projection function $p \in \Re^{N_x \times d}$ and $q \in \Re^{N_y \times d}$ such that the locations of x_i and y_j in k_i and t_j are close together as possible if $x_i \leftrightarrow y_j$. And that the resulting embedding $p^T X$ and $q^T Y$ preserve both global and local geometries of each manifold and the connections between them.

A. GLOBAL AND LOCAL STRUCTURES PRESERVING PCA FRAMEWORK

Principal Component Analysis (PCA) [40] is widely utilized to obtain low dimensional linear representations. We extend this idea to a penalty weight PCA to preserve noise-free global geometries. However, in many non-linear instances local information is very necessary. Thus, we preserve local geometries using multiple manifold embedding methods, different from the existing methods such as SSMA-FC that use single methods. We complement the varied representations (from these methods) to guarantee better local geometries are preserved in each manifold.

Also, having been inspired partly from the Graph-Laplacian PCA [41] method, where a Laplacian graph is combined with the traditional PCA, and from our recent works [42], [43] on dimension reduction. We thus take for instance the objective function of LPP as in eqn. (1):

$$\min_{w} w^T X L X^T w \quad s.t.\ w^T X D X^T w = 1 \tag{1}$$

and by adding the Lagrange multiplier to eqn. (1) with further derivatives, the following eigenvalue solution is obtained:

$$X L X^T w = \lambda (X D X^T w). \tag{2}$$

We reformulate by multiplying both sides of eqn. (2) by $(D^{\frac{1}{2}} X^T)(X D X^T)^{-1}$, together with algebraic transformations to obtain the following:

$$(D^{\frac{1}{2}} X^T)(X D X^T)^{-1}(X L X^T)(X D X^T)^{-1}(X D^{\frac{1}{2}}) (D^{\frac{1}{2}} X^T) w = \lambda (D^{\frac{1}{2}} X^T) w. \tag{3}$$

where $(D^{\frac{1}{2}} X^T)(X D X^T)^{-1}(X L X^T)(X D X^T)^{-1}(X D^{\frac{1}{2}})$, is a covariance matrix construction similar to that of PCA. From this we can see that manifold embedding methods such as LPP, NPE, and SPP are special forms of PCA that can preserve local structures.

Therefore, with this unified PCA and manifold embedding methods, we propose to construct a low-dimensional representation of a dataset X with intrinsic local and global structures, through the following function (4) with a generalized

eigen-value solution as eqn. (5):

$$\min_{u^T\delta u=1} \left\| X - X\delta^{\frac{1}{2}} uu^T \delta^{\frac{1}{2}} \right\|_F^2 + \alpha \sum_{g=1}^{L} \gamma_g \sum_{i,j=1}^{m} \left\| u_i - u_j \right\|_2^2 W_{g,i,j}. \quad (4)$$

$$\left(\alpha \sum_{g=1}^{L} \gamma_g L_g - \delta^{\frac{1}{2}} XX^T \delta^{\frac{1}{2}} \right) \quad u = \lambda \delta u. \quad (5)$$

where, $u = X^T w \in \Re^n$ refers to a generalization of the orthogonal vector $w \in \Re^m$ that considers data distribution in orthogonal projection to reconsider missing data points. α is a tradeoff parameter. $\delta = diag(\delta_1, \delta_2, \cdots, \delta_n)$ is a diagonal matrix which injects a penalty weight in each data point $(X_1, X_2, \cdots, X_n)^T$ to avoid outliers. γ_g is a regularization weight coefficient of the g^{th} manifold. The g^{th} graph laplacian matrix $L_g = D_g - W_g$. D_g and W_g are respectively the g^{th} diagonal and similarity weight matrices obtain from each of the manifold embedding methods such as LPP, NPE, LE, LSDA, and SPP.

B. OPTIMIZING MAPGL

Given prior l correspondence information, the similarity matrix $C^{xy} \in \Re^{m\times n}$ between the two manifolds is constructed as:

$$C_{ij}^{xy} = \begin{cases} 1 & \text{If } x_i \text{ is in correspondence with } x_j (i, j \in [1, l]) \\ 0 & \text{otherwise.} \end{cases}$$

Then applying our idea in eqn. (4), we propose to align manifolds through a novel PCA framework that preserves both global and local structures by minimizing the following cost function:

$$\begin{aligned} C(k,t) &= \mu A^s + A^x + A^y, \\ A^s &= \sum_{i=1}^{m}\sum_{j=1}^{n} \left\| k_i - t_j \right\|_2^2 C_{i,j}^{xy}, \\ A^x &= \left\| X - X\delta^{\frac{1}{2}} kk^T \delta^{\frac{1}{2}} \right\|_F^2 + \alpha \sum_{g=1}^{L} \gamma_g \sum_{i,j=1}^{m} \left\| k_i - k_j \right\|_2^2 W_{g,i,j}^x, \\ A^y &= \left\| Y - Y\delta^{\frac{1}{2}} tt^T \delta^{\frac{1}{2}} \right\|_F^2 + \phi \sum_{g=1}^{L} \beta_g \sum_{i,j=1}^{n} \left\| t_i - t_j \right\|_2^2 W_{g,i,j}^y. \end{aligned} \quad (6)$$

The first term A^s penalizes the difference between the embedding coordinates of X and Y. The last two terms, A^x and A^y, guarantee that both global and local geometries of each dataset are preserved in the embedding space. The μ, α, and ϕ are tradeoff parameters.

With further deductions and representing eqn. (6) in matrix form, the correspondence preserving term A^s can be rewritten as:

$$A^s = tr\left(kD^{xy}k^T - 2kC^{xy}t^T + tD^{yx}t^T \right). \quad (7)$$

where the diagonal matrices D^{xy} and D^{yx}, have $D_{ii}^{xy} = \sum_j^m C_{ij}^{xy}$ and $D_{jj}^{yx} = \sum_j^n C_{ij}^{yx}$ respectively. Also, the A^x and A^y can be represented as:

$$\begin{aligned} A^x &= tr\left(\alpha \sum_{g=1}^{L} \gamma_g \left(k \left(D_g^x - W_g^x \right) k^T \right) \right) - tr\left(k\delta^{\frac{1}{2}} XX^T \delta^{\frac{1}{2}} k^T \right) \\ A^x &= tr\left(k \left(\alpha \sum_{g=1}^{L} \gamma_g L_g^x - \delta^{\frac{1}{2}} XX^T \delta^{\frac{1}{2}} \right) k^T \right) \\ A^x &= tr\left(kG^x k^T \right). \end{aligned} \quad (8)$$

and similarly,

$$A^y = tr\left(tG^y t^T \right) \quad (9)$$

where $G^x = \left(\alpha \sum_{g=1}^{L} \gamma_g L_g^x - \delta^{\frac{1}{2}} XX^T \delta^{\frac{1}{2}} \right)$ and $G^y = \left(\phi \sum_{g=1}^{L} \beta_g L_g^y - \delta^{\frac{1}{2}} YY^T \delta^{\frac{1}{2}} \right)$

Thus the cost function in eqn. (6) can be rewritten as:

$$\begin{aligned} C(k,t) &= \mu.tr\left(kD^{xy}k^T - 2kC^{xy}t^T + tD^{yx}t^T \right) + tr\left(kG^x k^T \right) + tr\left(tG^y t^T \right) \\ &= tr\left[\begin{bmatrix} k & t \end{bmatrix} \begin{bmatrix} \mu D^{xy} + G^x & -\mu C^{xy} \\ -\mu C^{yx} & \mu D^{yx} + G^y \end{bmatrix} \begin{bmatrix} k^T \\ t^T \end{bmatrix} \right] \\ &= tr\left(FGF^T \right). \end{aligned} \quad (10)$$

where

$$F = \begin{bmatrix} k & t \end{bmatrix}, \; G = \begin{bmatrix} \mu D^{xy} + G^x & -\mu C^{xy} \\ -\mu C^{yx} & \mu D^{yx} + G^y \end{bmatrix},$$

$$D = \begin{bmatrix} \mu D^{xy} + \sum_{g=1}^{L} \gamma_g D_g^x & 0 \\ 0 & \mu D^{yx} + \sum_{g=1}^{L} \beta_g D_g^y \end{bmatrix}.$$

We further impose a constraint to remove arbitrary scaling factor in the embedding as follows:

$$\underset{F}{\text{argmin}} \; C(F) = \underset{F}{\text{argmin}} \; tr\left(FGF^T \right) \quad s.t.\; FDF^T = I. \quad (11)$$

Then by applying the Lagrange multiplier and taking partial derivatives, we get the following generalized eigenvalue solution:

$$GF^T = \lambda DF^T. \quad (12)$$

clearly, by computing the d eigenvectors $[F_1, \cdots, F_d]$ corresponding to the top m and the next n rows of the d smallest eigenvalues, the embedding coordinates k and t can be gotten.

It can be realized from cost function (10) that, the embedding results k and t are directly computed based on instances and not their respective mapping functions p and q. But this

poses a great difficulty in handling new data points. To overcome this challenge, we impose the constraints $k = p^T X$ and $t = q^T Y$ on function (10) resulting to the following:

$$C(p, q) = tr\left([p^T X \quad q^T Y] \ (G) \begin{pmatrix} X^T p \\ Y^T q \end{pmatrix} \right). \quad (13)$$

Let $M = \begin{pmatrix} X & 0 \\ 0 & Y \end{pmatrix}$ and $v = \begin{pmatrix} p \\ q \end{pmatrix}$, we can similarly obtain a generalized eigenvalue solution as

$$MGM^T v = \lambda MDM^T v. \quad (14)$$

where the linear mapping functions p and q are the top N_x and the next N_y rows of the d smallest eigenvectors $v_1, \cdots, v_d$.

C. OBTAINING PARAMETERS γ AND β IN MAPGL

This paper proposed a special PCA framework that also preserves local structure through multiple manifold embedding methods. We discuss how to optimally obtain parameters γ and β, which represent the weight coefficient vectors for the multiple manifolds of datasets X and Y, respectively.

For instance-level, given that L manifolds: $L_1^x, L_2^x, \cdots, L_L^x$, are used as in eqn. (6). We desire the value of γ_g which controls the influence of the g^{th} manifold in the proposed method. Thus, subject to $\sum_{g=1}^{L} \gamma_g = 1$, we add the Lagrange multiplier with respect to γ_g as follows:

$$\left(k \sum_{g=1}^{L} \gamma_g L_g^x k^T \right) + \lambda \left(1 - \sum_{g=1}^{L} \gamma_g \right). \quad (15)$$

Additionally, we extend γ_g to γ_g^r, where r is a parameter to control the weights of the multiple manifolds. Due to linear programming attain optimal solutions at extreme ends i.e. either $\gamma_g = 0$ or $\gamma_g = 1$, implying only one manifold will be selected different from our objective of complementing rich features from multiple manifolds. Thus, we set $r > 1$ to obtain a balance among multiple manifolds [44]. Taking partial derivatives of eqn. (15) while set to zero, we obtain the following:

$$\gamma_g = \frac{\left(\frac{1}{tr\left(k L_g^x k^T \right)} \right)^{\frac{1}{r-1}}}{\sum_{g=1}^{L} \left(\frac{1}{tr\left(k L_g^x k^T \right)} \right)^{\frac{1}{r-1}}}. \quad (16)$$

and in the same way for dataset Y we can deduce to:

$$\beta_g = \frac{\left(\frac{1}{tr\left(t L_g^y t^T \right)} \right)^{\frac{1}{r-1}}}{\sum_{g=1}^{L} \left(\frac{1}{tr\left(t L_g^y t^T \right)} \right)^{\frac{1}{r-1}}}. \quad (17)$$

For feature-level, we recall $k = p^T X$ and $t = q^T Y$. Similarly we can learn linear mapping functions p and q from eqns. (16) and (17) to respectively obtain γ_g and β_g as follows:

$$\gamma_g = \frac{\left(\frac{1}{tr\left(p^T X L_g^x X^T p \right)} \right)^{\frac{1}{r-1}}}{\sum_{g=1}^{L} \left(\frac{1}{tr\left(p^T X L_g^x X^T p \right)} \right)^{\frac{1}{r-1}}}. \quad (18)$$

$$\beta_g = \frac{\left(\frac{1}{tr\left(q^T Y L_g^y Y^T q \right)} \right)^{\frac{1}{r-1}}}{\sum_{g=1}^{L} \left(\frac{1}{tr\left(q^T Y L_g^y Y^T q \right)} \right)^{\frac{1}{r-1}}}. \quad (19)$$

Algorithm 1 The Proposed MAPGL Method

Input: X, Y, and L
Output: F or v
Parameters: μ, α, ϕ and r
Initialize:
- normalize X and apply PCA to reduce the dimensions
-set $\gamma = (1/L, 1/L, \cdots, 1/L)^T$,
$\beta = (1/L, 1/L, \cdots, 1/L)^T$
-construct diagonal matrices $\{D_g^x\}_{g=1}^L$, $\{D_g^y\}_{g=1}^L$, D^{xy}
-construct similarity matrices $\{W_g^x\}_{g=1}^L$, $\{W_g^y\}_{g=1}^L$, C^{xy}
-construct $\{L_g^x\}_{g=1}^L$, $\{L_g^y\}_{g=1}^L$, and δ.
for Instance-level (I)
while loss not converged **do**
  construct matrices G, D and M
  obtain F by eqn. (12)
  update γ and β according to eqns. (16) and (17)
  compute loss from eqn. (11)
end while
for Feature-level (F)
while loss not converged **do**
  construct matrices G, D and M
  obtain v by eqn. (14)
  update γ and β according to eqns. (18) and (19)
  compute loss from eqn. (13)
end while

Algorithm 1 is a summary of the proposed method.

IV. EXPERIMENTS

In this section, we undertake several experiments on manifold alignment to evaluate the performance of our MAPGL method in comparison with SSMA-FC [22], SSMA [5], PAMA [4], and UNMA [6] methods. A total of four (4) real world datasets are used such as, Glutaredoxin protein PDB-1G7O, COIL-100, UMIST, and WIKI Text-Image. In our experiments, MAPGL method is performed at feature-level and instance-level where applicable which we represent as MAPGL(F) and MAPGL(I) respectively.

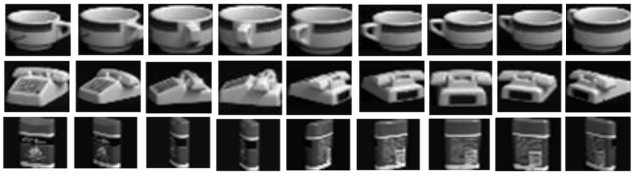

FIGURE 1. Sample images of objects 10, 30, 90 of COIL-100 dataset.

A. DATASETS AND EXPERIMENTAL SETTINGS

The 3D structure of Glutaredoxin protein PDB-1G7O [45] consists of 21 models of which each model is made up of 215 amino acids. We formed two datasets, X and Y of sizes 3×215 using the 1^{st} and the 21^{st} models respectively. The 3D structures of these datasets are illustrated in Fig.2.

The COIL-100[1] dataset [46] is maintained by the image library of Columbia University, consisting 100 color images of different objects. Each object has 72 images taken from different angles at intervals of 5 degrees over a dark background. We resize each image to 32×32 pixels of 256 grayscale. We present some images from this dataset in Fig.1.

The UMIST[2] face dataset has a total of 564 images contributed by 20 people. Each individual contributed from 19 to 36 images that span from profile to frontal views of poses. The subjects include race, sex, and appearance. For our experiments we crop and reshape the images to 112×92 (i.e., 10304) dimensions. We illustrate part of these images in Fig. 7.

The Wiki Text-Image[3] dataset [47] is a collection of articles in Wikipedia. This collection is over 29 categories of 2669 articles continually reviewed. A category label is assigned to each featured article image and text. Considering only the top 10 populated articles having at least 150 instances in each class, a corpus is made consisting 2866 multimedia documents: art, biology, geography, history, literature, media, music, royalty, sport and warfare. There are two multiple features; the 10-D Latent Dirichlet allocation base text features and 128-D SIFT Histogram image feature.

The propose MAPGL method has parameters k, μ, α, ϕ and r which are set as follows: the size of the k-nearest-neighbors [48] parameter k is set as 3. The regularization parameters μ, α, ϕ are chosen from the set $(0.1, 0.2, \cdots, 0.9)$. The parameter r which controls the weights of the multiple manifolds is chosen from $(2, 4, \cdots, 14)$. The number of manifold embedding methods in this paper is 4, i.e. $L = 4$. For any parameter in the comparative algorithms different from above is set as provided by the authors. The experiments are repeated for each manifold alignment algorithm through the above ranges and the best results in each case reported.

[1]http://www.cad.zju.edu.cn/home/dengcai/Data/MLData.html
[2]http://web.mit.edu/emeyers/www/face_databases.html
[3]http://www.svcl.ucsd.edu/projects/crossmodal/

B. PROTEIN MANIFOLDS ALIGNMENT

In this subsection, the performance of the proposed MAPGL algorithm on aligning the 3D structures of model 1 and model 21 of the Glutaredoxin PDB-1G7O [45] is demonstrated. In our experiments we further rescaled the data matrix of model 1(X) as $X = X/4$ to obtain a different scale for testing. We illustrate these models using 3D structures (Fig.2(a) model 1, Fig.2(b) model 21, Fig.2(c) rescaled model 1 and model 21.

The proposed MAPGL method together with the comparative manifold alignment methods, PAMA, UNMA, SSMA, SSMA-FC are use to align the protein datasets, while maintaining a fix correspondence of 5 amino acids. The alignment performances of all the methods are plotted in 3D in Fig. 3. It can be noticed that the proposed MAPGL method demonstrates much improvement over the rest of the comparative methods. Semi-supervised PAMA and SSMA perform not quite well due to their requirements of larger correspondence sizes. UNMA which does not require prior correspondence, but due to the preservation of local geometries consider neighborhood relationships, it is able to outperform PAMA and SSMA. The SSMA-FC method which underperforms the proposed MAPGL even with the few correspondences is due to the following: (1) the proposed MAPGL has advantages of preserving more refined local structures with multiple manifolds embedding methods than the SSMA-FC that makes use of only one manifold embedding method. (2) MAPGL also preserves global structure in a balance with the local structure to achieve the final structure, this is absent in SSMA-FC.

C. ROTATED OBJECTS ALIGNMENT

Using the COIL-100 dataset, we test the performance of the proposed MAPGL on image matching task. We test for sensitivity of the algorithm with different correspondence information as well as reduced dimensions. These experiments are done on four selected objects such as 10, 30, 60 and 90, represented in this paper as obj10, etc. Each of the manifold alignment algorithms including the proposed and comparative methods are made to align each object against the rest. Thus we had six (6) sets such as obj10&30, obj10&60, obj10&90, obj30&60, obj30&90, and obj60&90. In each of the sets we had three (3) different experiments with correspondences of $c = 2$, $c = 6$, and $c = 12$. The various methods MAPGL, PAMA, SSMA, UNMA and SSMA-FC are separately used to obtain a common embedding space by projecting both the source (X) and the target (Y) datasets. To match instance x_i to y_j, we take the absolute difference of their degrees of rotation such as $|\theta_{x_i} - \theta_{y_j}|$. And then we compute the average of the absolute difference over all the source instances x_i, to obtain the matching error of alignment.

Table 1 contains the matching errors of aligning the different objects with correspondences of 2, 6, and 12 by the six (6) manifold alignment algorithms. From Table 1, it can be seen that in the overall average, UNMA performed poorly, but led SSMA and PAMA in obj10&30 and obj10&60 respectively. SSMA, PAMA and SSMA-FC are averagely a little

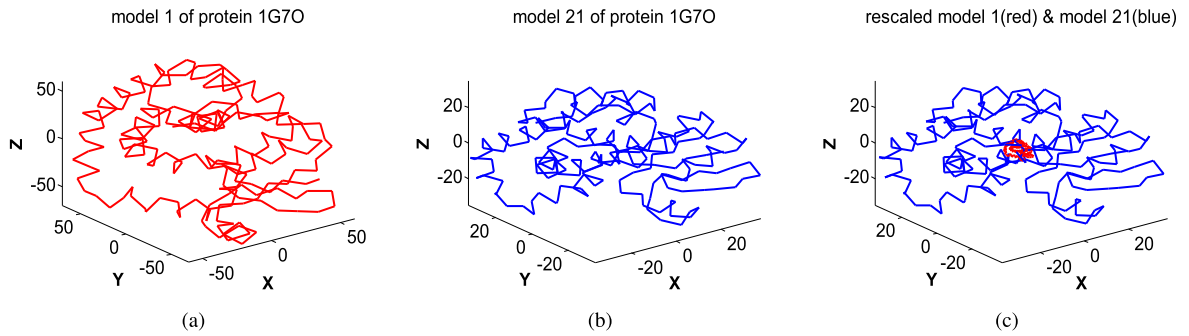

FIGURE 2. Structures of Glutaredoxin PDB-1G7O dataset (a) model 1, (b) model 21, and (c) rescaled model 1 and model 21.

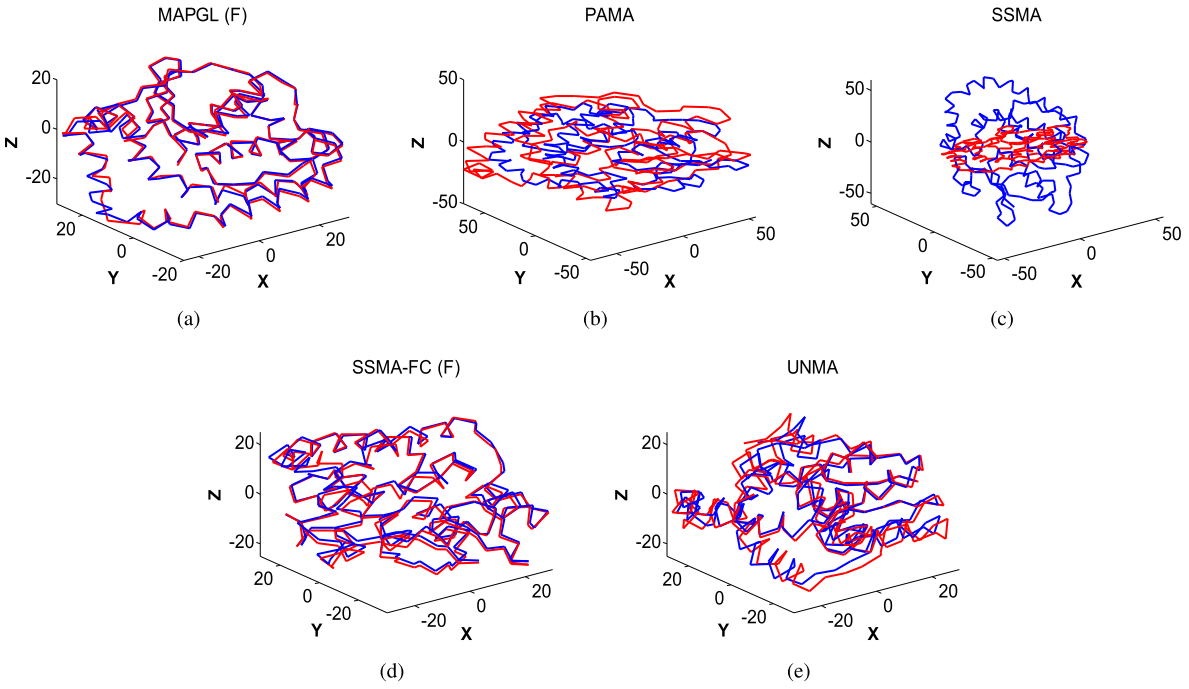

FIGURE 3. Structure alignment of models 1 and 21 of Glutaredoxin PDB-1G7O dataset by (a) MAPGL, (b) PAMA, (c) SSMA, (d) SSMA-FC(F), and (e) UNMA methods.

better in the experiments and saw much improvements in higher correspondence, $c = 12$. The proposed MAPGL(F) and MAPGL(I) obtain the best alignment results in turns throughout. It can be seen that MAPGL can align obj10&30 best than the rest of the objects with an error of less than 4° when $c = 12$. Also, aside UNMA which does not require prior correspondence, the rest of the comparative methods are very sensitive to increase in correspondence, but the proposed MAPGL is slightly sensitive.

Also, in Fig. 4 we illustrate the trend of performance of the algorithms in aligning obj30&60 in different dimensions and correspondences. From Fig. 4, it can be observed that the comparative UNMA, SSMA, PAMA, and SSMA-FC are very unstable in different dimensions and correspondences. The proposed MAPGL(F) and MAPGL(I) outperform all the comparative methods and are very stable in different dimensions and correspondences. This means the computation time of our method will be enhanced since any dimension can be selected instead of it being searched.

D. HEAD POSE IMAGES ALIGNMENT

Experiments in this section were performed on aligning head pose images using UMIST dataset. For the purpose of this experiment, we selected the first and the second persons considering pose angles from 3° to 90° with 3° increments to form two datasets. Each dataset (one as the source and the other as the target) contains 30 samples of dimensions 10304.

We apply the manifold alignment methods MAPGL, PAMA, SSMA, UNMA and SSMA-FC to project the source (X) and target (Y) datasets to a common embedding space. Then match an instance x_i to y_j, by computing the absolute difference of their degrees of variation such as $|\theta_{x_i} - \theta_{y_j}|$. And finally the average of the absolute difference over all the source instances x_i, to obtain the alignment

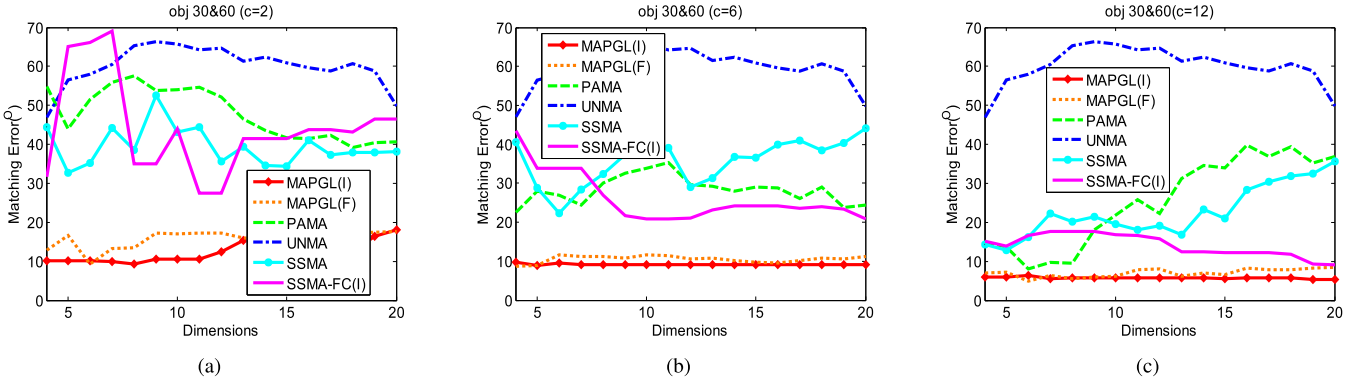

FIGURE 4. The trend of matching alignment errors in different dimensions for the various algorithms on obj30 & obj60 of COIL-100 dataset in correspondences of (a) c=2, (b) c=6, (c) c=12.

TABLE 1. The matching errors (°) of alignment for the various algorithms on compared objects 10,30,60,90 of COIL-100 dataset.

		Obj10&30	Obj10&60	Obj10&90	Obj30&60	Obj30&90	Obj60&90
c=2	MAPGL(F)	6.70	13.17	11.77	**9.27**	12.71	10.17
	MAPGL(I)	**6.05**	**12.65**	**10.57**	9.31	**10.07**	**6.35**
	UNMA	62.78	41.08	37.03	46.97	50.08	26.17
	SSMA	67.56	35.08	38.36	32.78	35.64	30.60
	PAMA	51.75	46.25	37.31	39.08	36.69	26.86
	SSMA-FC(I)	34.56	38.97	23.18	27.44	30.11	25.68
c=6	MAPGL(F)	7.73	10.49	**8.78**	**8.77**	**9.53**	9.53
	MAPGL(I)	**6.27**	**9.17**	9.53	8.99	9.76	**5.20**
	UNMA	62.78	41.08	37.03	46.97	50.08	26.17
	SSMA	41.72	23.33	22.11	22.22	28.22	11.44
	PAMA	36.50	24.42	22.63	22.61	21.08	16.33
	SSMA-FC(I)	22.64	22.94	11.78	20.81	21.83	13.92
c=12	MAPGL(F)	**3.68**	6.56	5.68	**4.90**	**8.58**	6.18
	MAPGL(I)	3.79	**6.13**	**3.88**	5.33	8.83	**4.27**
	UNMA	62.78	41.08	37.03	46.97	50.08	26.17
	SSMA	18.67	17.58	10.92	12.83	17.39	8.89
	PAMA	20.04	5.69	9.92	7.94	13.71	8.04
	SSMA-FC(I)	5.08	8.7	5.83	9.17	10.50	5.78

TABLE 2. The alignment matching errors (°) for the various algorithms on UMIST dataset.

	MAPGL (F)	MAPGL (I)	UNMA	SSMA	PAMA	SSMA -FC(I)
c=2	8.2	**7.7**	25.75	23	24.5	19
c=4	4.8	**4.6**	25.75	11	18	17
c=7	**2.8**	4.33	25.75	8.25	8	9.5

matching errors. We report the performance of the various methods in aligning images of persons 1 and 2 in varying correspondences in Table 2. From Table 2, it can be seen that UNMA which does not require correspondence, performs poorly among all methods especially in higher correspondence. SSMA, PAMA, and SSMA-FC(I) perform better in the higher correspondence of 7 than in the lower. The proposed MAPGL(F) and MAPGL(I) can be seen to outperform all the comparative methods in all correspondences. Also, MAPGL can be seen as less sensitive to increase in correspondence: since from $c = 2$ to $c = 7$, MAPGL(I) marginally improved by 3.37 as opposed to SSMA by 14.75, PAMA by 16.5, and SSMA-FC(I) by 9.5. To show sensitivity of the methods to dimensionality size, we illustrate their performance in different reduced dimensions varying from 4 to 20 in Fig. 5. From this figure the proposed methods clearly outperform the comparative manifold alignment methods in all dimensions across the different correspondences. In addition the proposed methods are most stable, specifically, MAPGL(I) is more stable than MAPGL(F). This indicates that the proposed method can preserve both global and local structures at instance-level better than at feature-level.

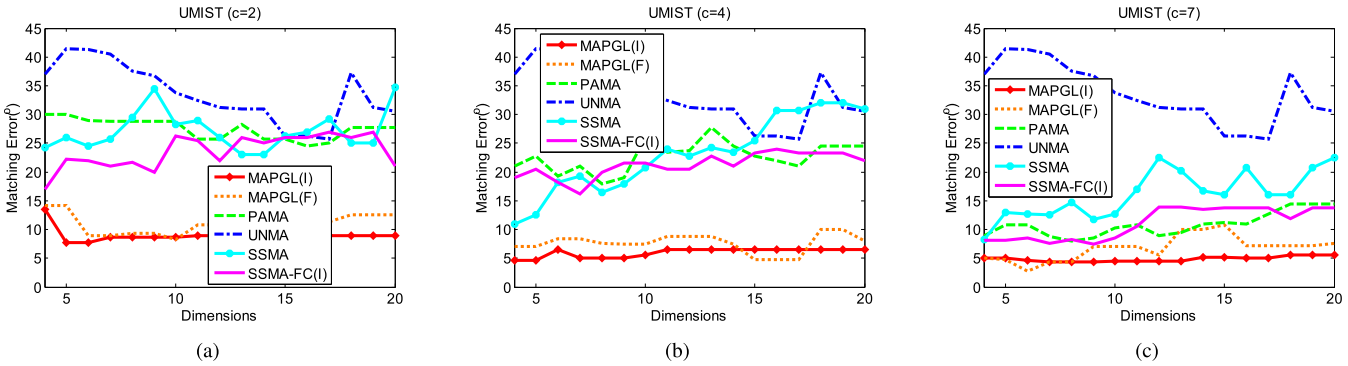

FIGURE 5. The trend of matching alignment errors in different dimensions for the various algorithms on UMIST dataset in correspondences of (a)c=2 (b)c=4 (c)c=7.

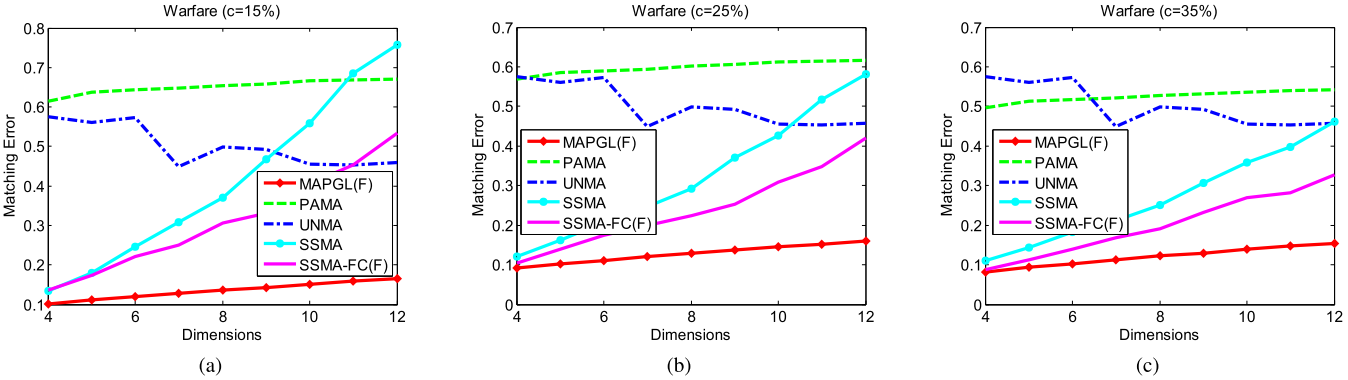

FIGURE 6. The trend of matching alignment errors(%) in different dimensions for the various algorithms on warfare of Wiki Image-Text dataset in correspondences of (a)c=15% (b)c=25% (c)c=35%.

FIGURE 7. The pair-wise alignment matching results on UMIST dataset (a) source images, (b) MAPGL(F), (c) MAPGL(I), (d) UNMA, (e) SSMA, (f) PAMA, and (g) SSMA-FC(I).

Furthermore, we show the source images with pose angles from 3° to 90° in increments of 6° in Fig. 7(a). In Fig. 7 we compare the source images in (a) with the matching target images results of MAPGL(F), MAPGL(I), UNMA, SSMA, PAMA, and SSMA-FC(I) labeled as (b) to (g) respectively. A correspondence of $c = 4$ is used and a mismatched

TABLE 3. The alignment matching errors (%) for the various algorithms on Wiki Image-Text dataset.

		warfare	media	sport
c=15%	MAPGL(F)	**10.07**	**3.71**	**13.42**
	UNMA	57.53	35.25	61.65
	SSMA	13.40	8.89	27.39
	PAMA	61.52	23.47	60.43
	SSMA-FC(F)	13.56	7.50	22.25
c=25%	MAPGL(F)	**9.26**	**3.21**	**12.22**
	UNMA	57.53	35.25	61.65
	SSMA	12.02	7.79	24.18
	PAMA	56.81	23.22	60.41
	SSMA-FC(F)	10.40	6.41	20.38
c=35%	MAPGL(F)	**8.10**	**2.36**	**11.17**
	UNMA	57.53	35.25	61.65
	SSMA	10.98	4.97	18.99
	PAMA	49.76	23.43	60.47
	SSMA-FC(F)	8.71	3.83	15.45

image (with angle error more than 5°) is marked red. From Fig. 7, it can be seen that the proposed methods can find most matches than the rest of the comparative methods while UNMA which does not need correspondence obtains the fewest matches.

E. IMAGE AND TEXT ALIGNMENT

In this section, we conduct experiments to align image and text by the manifold alignment methods using the Wiki Image-Text dataset. We use the Latent Dirichlet Allocation base text features and SIFT Histogram image features extracted from this dataset as the source and target. We select three (3) of the populated articles such as warfare, media, and sport for the experiments with correspondences of 15%, 25%, and 35%.

Each manifold alignment method is used to project the source and target datasets to a common embedding space. For a selected sample of the embedding space, a Euclidean distance between x_i of the source and that of y_j of the target is computed. Then the matching error of alignment is obtained by the average of the Euclidean distances over all x_i. The instance level of our method and the others fail to implement successfully, due to the complexity of this dataset. We report the results of the matching errors of alignment by the various algorithms in Table 3. From this table, UNMA once again averagely underperform all the methods. PAMA followed with the worst performance especially under warfare and sport. SSMA and SSMA-FC(F) are seen with good results with the latter leading marginally in most instances. The proposed MAPGL(F) outperforms all the comparative methods, especially in lower correspondence of $c = 15\%$, where a significant margin of more than 3% is obtained.

We further show the performance of the algorithms in different dimensions of the embedding space with few

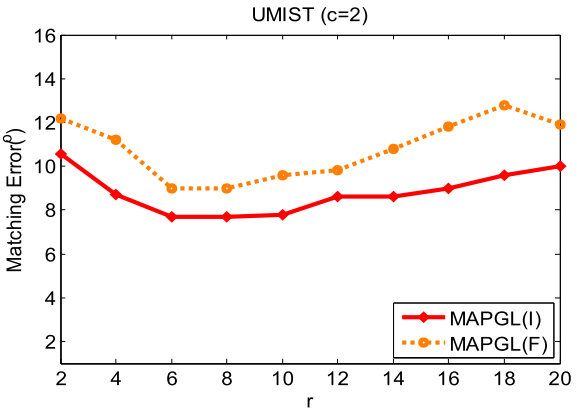

FIGURE 8. The matching errors (°) of alignment in different values of r on UMIST dataset.

correspondences of 15%, 25%, and 35% in Fig. 6. From this figure, UNMA is the most stable even though with the worst performance, because it does not depend on correspondence information. PAMA, SSMA, and SSMA-FC(F) are very unstable, while the proposed MAPGL(F) is more stable followed by UNMA. This means the proposed MAPGL(F) is robust and less sensitive to correspondence information.

F. EFFECT OF PARAMETERS IN MAPGL

In our experiments, the optimal values of the parameters were determined through cross validation. And from this we realized that, when the regularization parameters μ, α, ϕ are set $\leq$ 0.9, did not have any significant effect on the alignment result. But the control parameter r (which determines the weight of multiple manifolds) had an influence on the alignment result. Therefore, we discuss the influence of parameter r, by testing with varied values from 2 to 20 (in steps of 2) on the UMIST dataset. The correspondence was set as $c = 2$, and the regularization parameters $\mu = 0.2$, $\alpha = 0.5$, and $\phi = 0.6$. The matching errors of alignment in varying values of r are presented in Fig. 8. It can be seen that the errors in alignment are low in the range of 6 to 14 of r, while attaining stable and minimum errors at 6, and 8. Thus, for high performance of the proposed MAPGL in general, the control parameter r should be set to 6 or 8.

V. CONCLUSIONS

In this paper, a novel semi-supervised manifold alignment algorithm is proposed that can preserve global and local structures of multiple datasets. A close-form solution to an optimization problem is presented. This achieves a latent low-dimensional space by matching pair-wise correspondence and preserving both global and local structures through a novel PCA framework. This PCA framework is a unified penalty weight PCA and multiple manifold embedding methods with the capability of suppressing noise leading to better structural stability. This paper reveals that, manifold embedding methods are special forms of PCA. And optimally complementing multiple local structures and global structures can improve the alignment results of multiple datasets.

Extensive manifold alignment experiments in four (4) datasets reveal the significant improvements of the proposed MAPGL over the manifold alignment methods such as, PAMA, UNMA, SSMA, and SSMA-FC. In the future we shall explore to eliminate the reliance on few pair-wise correspondences.

REFERENCES

[1] B.-K. Bao, C. Xu, W. Min, and M. S. Hossain, "Cross-platform emerging topic detection and elaboration from multimedia streams," *ACM Trans. Multimedia Comput. Commun. Appl.*, vol. 11, no. 4, pp. 1–21, 2015.

[2] T. Boucher, C. J. Carey, S. Mahadevan, and M. D. Dyar, "Aligning mixed manifolds," in *Proc. 29th AAAI Conf. Artif. Intell.*, 2015, pp. 1–7.

[3] A. L'heureux, K. Grolinger, H. F. Elyamany, and M. A. Capretz, "Machine learning with big data: Challenges and approaches," *IEEE Access*, vol. 5, pp. 777–797, 2017.

[4] C. Wang and S. Mahadevan, "Manifold alignment using procrustes analysis," in *Proc. 25th Int. Conf. Mach. Learn.*, 2008, pp. 1120–1127.

[5] J. Ham, D. D. Lee, and L. K. Saul, "Semisupervised alignment of manifolds," in *Proc. 10th Int. Workshop Artif. Intell. Statist.*, 2005, pp. 120–127.

[6] C. Wang and S. Mahadevan, "Manifold alignment without correspondence," in *Proc. Int. Joint Conf. Artif. Intell.* Pasadena, CA, USA: Morgan Kaufmann, Jul. 2009, pp. 1273–1278.

[7] G. Niu and Z. Ma, "Local non-linear alignment for non-linear dimensionality reduction," *IET Comput. Vis.*, vol. 11, no. 5, pp. 331–341, 2017.

[8] X. Li, J. Lv, W. Xi, and Y. Xin, "A semi-supervised manifold alignment algorithm and an evaluation method based on local structure preservation," *Neurocomputing*, vol. 224, pp. 195–203, Feb. 2017.

[9] C. Wang and S. Mahadevan, "Manifold alignment preserving global geometry," in *Proc. 23rd Int. Joint Conf. Artif. Intell. (IJCAI)*, 2013, pp. 1743–1749.

[10] X. Peng, J. Feng, S. Xiao, W.-Y. Yau, J. T. Zhou, and S. Yang, "Structured autoencoders for subspace clustering," *IEEE Trans. Image Process.*, vol. 27, no. 10, pp. 5076–5086, Oct. 2018.

[11] X. Peng, C. Lu, Z. Yi, and H. Tang, "Connections between nuclear-norm and Frobenius-norm-based representations," *IEEE Trans. Neural Netw. Learn. Syst.*, vol. 29, no. 1, pp. 218–224, Jan. 2018.

[12] X.-Y. Jing *et al.*, "Super-resolution person re-identification with semi-coupled low-rank discriminant dictionary learning," *IEEE Trans. Image Process.*, vol. 26, no. 3, pp. 1363–1378, Mar. 2017.

[13] X.-Y. Jing and D. Zhang, "A face and palmprint recognition approach based on discriminant DCT feature extraction," *IEEE Trans. Syst., Man, Cybern. B, Cybern.*, vol. 34, no. 6, pp. 2405–2415, Dec. 2004.

[14] X. Peng, J. Lu, Z. Yi, and R. Yan, "Automatic subspace learning via principal coefficients embedding," *IEEE Trans. Cybern.*, vol. 47, no. 11, pp. 3583–3596, Nov. 2017.

[15] W. Liu, H. Zhang, D. Tao, Y. Wang, and K. Lu, "Large-scale paralleled sparse principal component analysis," *Multimedia Tools Appl.*, vol. 75, no. 3, pp. 1481–1493, 2013.

[16] C. Moulin, C. Largeron, C. Ducottet, M. Géry, and C. Barat, "Fisher linear discriminant analysis for text-image combination in multimedia information retrieval," *Pattern Recognit.*, vol. 47, no. 1, pp. 260–269, 2014.

[17] X. Zhu, X. Li, S. Zhang, C. Ju, and X. Wu, "Robust joint graph sparse coding for unsupervised spectral feature selection," *IEEE Trans. Neural Netw. Learn. Syst.*, vol. 28, no. 6, pp. 1263–1275, Jun. 2017.

[18] J. Gui, Z. Sun, W. Jia, R. Hu, Y. Lei, and S. Ji, "Discriminant sparse neighborhood preserving embedding for face recognition," *Pattern Recognit.*, vol. 45, no. 8, pp. 2884–2893, Aug. 2012.

[19] Z. K. Malik, A. Hussain, and J. Wu, "An online generalized eigenvalue version of laplacian eigenmaps for visual big data," *Neurocomputing*, vol. 173, pp. 127–136, Jan. 2016.

[20] J. Lu and Y. P. Tan, "Regularized locality preserving projections and its extensions for face recognition," *IEEE Trans. Syst., Man, Cybern. B, Cybern.*, vol. 40, no. 3, pp. 958–963, Jun. 2010.

[21] X. Zhu, S. Zhang, R. Hu, Y. Zhu, and J. Song, "Local and global structure preservation for robust unsupervised spectral feature selection," *IEEE Trans. Knowl. Data Eng.*, vol. 30, no. 3, pp. 517–529, Mar. 2018.

[22] J. Wang, X. Zhang, X. Li, and J. Du, "Semi-supervised manifold alignment with few correspondences," *Neurocomputing*, vol. 230, pp. 322–331, Mar. 2017.

[23] J. H. Ham, D. D. Lee, and L. K. Saul, "Learning high dimensional correspondences from low dimensional manifolds," in *Proc. 20th Int. Conf. Mach. Learn.*, vol. 8, 2003, pp. 1–10.

[24] S. Tan, Z. Guan, D. Cai, X. Qin, J. Bu, and C. Chen, "Mapping users across networks by manifold alignment on hypergraph," in *Proc. AAAI*, vol. 14, 2014, pp. 159–165.

[25] W. Zhao *et al.*, "Learning to map social network users by unified manifold alignment on hypergraph," *IEEE Trans. Neural Netw. Learn. Syst.*, vol. 29, no. 12, pp. 5834–5846, Dec. 2018.

[26] M. Zhou, Y. Tang, W. Nie, L. Xie, and X. Yang, "GrassMA: Graph-based semi-supervised manifold alignment for indoor WLAN localization," *IEEE Sensors J.*, vol. 17, no. 21, pp. 7086–7095, Nov. 2017.

[27] G. Zhang, J. Chen, G. Su, and C. Ou, "Comparisons of local methods for face alignment," *IET Comput. Vis.*, vol. 10, no. 7, pp. 728–735, 2016.

[28] J. Verbeek, "Learning nonlinear image manifolds by global alignment of local linear models," *IEEE Trans. Pattern Anal. Mach. Intell.*, vol. 28, no. 8, pp. 1236–1250, Aug. 2006.

[29] H. L. Yang and M. M. Crawford, "Learning a joint manifold with global-local preservation for multitemporal hyperspectral image classification," in *Proc. IEEE Int. Geosci. Remote Sens. Symp. (IGARSS)*, Jul. 2013, pp. 1047–1050.

[30] D. Tuia, M. Volpi, M. Trolliet, and G. Camps-Valls, "Semisupervised manifold alignment of multimodal remote sensing images," *IEEE Trans. Geosci. Remote Sens.*, vol. 52, no. 12, pp. 7708–7720, Dec. 2014.

[31] Y. Qian, D. Liao, and J. Zhou, "Manifold alignment based color transfer for multiview image stitching," in *Proc. 20th IEEE Int. Conf. Image Process. (ICIP)*, Sep. 2013, pp. 1341–1345.

[32] L. Xiong, F. Wang, and C. Zhang, "Semi-definite manifold alignment," in *Proc. Eur. Conf. Mach. Learn.* Berlin, Germany: Springer, 2007, pp. 773–781.

[33] X. Wang, J. Ren, and S. Liu, "Distribution adaptation and manifold alignment for complex processes fault diagnosis," *Knowl.-Based Syst.*, vol. 156, pp. 100–112, Sep. 2018.

[34] Y. Zhao *et al.*, "Multi-view manifold learning with locality alignment," *Pattern Recognit.*, vol. 78, pp. 154–166, Jun. 2018.

[35] Z. Li, X.-Y. Jing, X. Zhu, H. Zhang, B. Xu, and S. Ying, "On the multiple sources and privacy preservation issues for heterogeneous defect prediction," *IEEE Trans. Softw. Eng.*, to be published.

[36] X.-Y. Jing, F. Wu, X. Dong, and B. Xu, "An improved SDA based defect prediction framework for both within-project and cross-project class-imbalance problems," *IEEE Trans. Softw. Eng.*, vol. 43, no. 4, pp. 321–339, Apr. 2017.

[37] W. Fei, X.-Y. Jing, S. Ying, S. Jing, and Y. Sun, "Cross-project and within-project semisupervised software defect prediction: A unified approach," *IEEE Trans. Rel.*, vol. 67, no. 2, pp. 581–597, Jun. 2018.

[38] X. Li, S. Lin, S. Yan, and D. Xu, "Discriminant locally linear embedding with high-order tensor data," *IEEE Trans. Syst., Man, Cybern. B, Cybern.*, vol. 38, no. 2, pp. 342–352, Apr. 2008.

[39] Y. Yuan, L. Mou, and X. Lu, "Scene recognition by manifold regularized deep learning architecture," *IEEE Trans. Neural Netw. Learn. Syst.*, vol. 26, no. 10, pp. 2222–2233, Oct. 2015.

[40] H. Abdi and L. J. Williams, "Principal component analysis," *Wiley Interdiscipl. Rev., Comput. Statist.*, vol. 2, no. 4, pp. 433–459, 2010.

[41] B. Jiang, C. Ding, B. Luo, and J. Tang, "Graph-Laplacian PCA: Closed-form solution and robustness," in *Proc. Comput. Vis. Pattern Recognit.*, Jun. 2013, pp. 3492–3498.

[42] T. A. Abeo, X.-J. Shen, J.-P. Gou, Q.-R. Mao, B.-K. Bao, and S. Li, "Dictionary-induced least squares framework for multi-view dimensionality reduction with multi-manifold embeddings," *IET Comput. Vis.*, vol. 13, no. 2, pp. 97–108, 2019.

[43] T. A. Abeo, X.-J. Shen, B.-K. Bao, Z.-J. Zha, and J. Fan, "A generalized multi-dictionary least squares framework regularized with multi-graph embeddings," *Pattern Recognit.*, vol. 90, pp. 1–11, Jan. 2019.

[44] M. Karasuyama and H. Mamitsuka, "Multiple graph label propagation by sparse integration," *IEEE Trans. Neural Netw. Learn. Syst.*, vol. 24, no. 12, pp. 1999–2012, Dec. 2013.

[45] H. M. Berman *et al.*, "The protein data bank and the challenge of structural genomics," *Nature Struct. Biol.*, vol. 7, no. 2, p. 957, 2000.

[46] S. A. Nene, S. K. Nayar, and H. Murase, "Columbia object image library (COIL-100)," Columbia Univ., New York City, NY, USA, Tech. Rep. CUCS-006-96, 1996.

[47] N. Rasiwasia *et al.*, "A new approach to cross-modal multimedia retrieval," in *Proc. Int. Conf. Multimedia*, 2010, pp. 251–260.

[48] S. Zhang, X. Li, M. Zong, X. Zhu, and D. Cheng, "Learning k for kNN classification," *ACM Trans. Intell. Syst. Technol.*, vol. 8, no. 3, p. 43, 2017.

TIMOTHY APASIBA ABEO received the B.Sc. degree in computer science and the M.Sc. degree in information technology from the Kwame Nkrumah University of Science and Technology (KNUST), Ghana, in 2008 and 2015, respectively. He is currently pursuing the Ph.D. degree in computer applied technology with Jiangsu University, China.

He is also a Lecturer with the Computer Science Department, School of Applied Science, Tamale Technical University, Ghana. His research interests include pattern recognition, multimedia analysis and retrieval, and machine learning.

XIANG-JUN SHEN received the M.S. degree in computer science from Jiangsu University, China, in 2003, and the Ph.D. degree in automation from the University of Science and Technology, China, in 2006. He is currently a Professor with the Department of Software Engineering, School of Computer Science and Communication Engineering, Jiangsu University. His research interests include cross multimedia analysis, computer vision, pattern recognition, and statistical machine learning. He is a member of the ACM and the CCF.

ERNEST DOMANAANMWI GANAA received the B.Sc. degree in computer science and the M.Sc. degree in information technology from the Kwame Nkrumah University of Science and Technology (KNUST), Ghana, in 2008 and 2015, respectively. He is currently pursuing the Ph.D. degree in computer applied technology with Jiangsu University, China. He is also a Lecturer with the ICT Department, School of Applied Science, Wa Polytechnic, Ghana. His research interests include machine learning, pattern recognition, and dimensionality reduction.

QIAN ZHU received the B.S. degree in computer application technology from the Jiangsu University of Science and Technology, in 2000, and the Ph.D. degree in computer science from Jiangsu University, in 2011, where she is currently an Associate Professor with the School of Computer Science and Communication Engineering. Her research interests include multimedia analysis, machine learning, and natural language processing.

BING-KUN BAO received the Ph.D. degree in control theory and control application from the University of Science and Technology of China, Hefei, China, in 2009. From 2009 to 2011, she was a Research Engineer of electrical and computer engineering with the National University of Singapore, Singapore. She is currently a Professor with the College of Telecommunications and Information Engineering, Nanjing University of Posts and Telecommunications, Jiangsu, China. She is a member of the IEEE and the ACM.

ZHENG-JUN ZHA received the B.E. degree in automation and the Ph.D. degree in pattern recognition and intelligent system from the University of Science and Technology of China (USTC), Hefei, China, in 2004 and 2009, respectively. He is currently a Professor with the School of Information Science and Technology, USTC. He has published over 100 book chapters and international journal and conference papers in these areas, including TMM, TCSVT, TOMCCAP, TIP, ACM MM, CVPR, and SIGIR. His current research interests include multimedia content analysis and retrieval, computer vision, and social media analysis. He is a member of the IEEE and the ACM. He received the Best Paper Award from the ACM International Conference on Multimedia (ACM MM), in 2009, and the Best Demo Runner-Up Award from ACM MM 2012. He has served as the Program Co-Chair, the Special Session Co-Chair, the Workshop Co-Chair, the Demo Co-Chair, and the Area Chair for various prestigious multimedia conferences. He has been serving as a Reviewer for more than 30 major international journals and as a Program Committee member for many prestigious conferences.